Tuning the Microenvironment: Click-Crosslinked Hyaluronic Acid-Based Hydrogels Provide a Platform for Studying Breast Cancer Cell Invasion

*Stephanie A. Fisher, Priya N. Anandakumaran, Shawn C. Owen, and Molly S. Shoichet**

A big challenge in cell culture is the non-natural environment in which cells are routinely screened, making in vivo phenomena, such as cell invasion, difficult to understand and predict. To study cancer cell invasion, extracellular matrix (ECM) analogs with decoupled mechanical and chemical properties are required. Hyaluronic acid (HA)-based hydrogels crosslinked with matrix-metalloproteinase (MMP)-cleavable peptides are developed to study MDA-MB-231 breast cancer cell invasion. Hydrogels are synthesized by reacting furan-modified HA with bismaleimide peptide crosslinkers in a Diels–Alder click reaction. This new hydrogel takes advantage of the biomimetic properties of HA, which is overexpressed in breast cancer, and eliminates the use of nonadhesive crosslinkers, such as poly(ethylene glycol) (PEG). The crosslink (mechanical) and ligand (chemical) densities are varied independently to evaluate the effects of each parameter on cell migration. Increased crosslink density correlates with decreased MDA-MB-231 cell invasion whereas incorporation of MMP-cleavable sequences within the peptide crosslinker enhances invasion. Increasing the ligand density of pendant GRGDS groups induces cell proliferation, but has no significant impact on invasion. By independently tuning the mechanical and chemical environment of ECM mimetic hydrogels, a platform is provided that recapitulates variable tissue properties and elucidates the role of the microenvironment in cancer cell invasion.

1. Introduction

The role of the extracellular matrix (ECM) in cancer cell invasion is not well understood. The microenvironment is a complex composition of structural ECM proteins, signaling molecules, and stromal cells, providing dynamic signals which influence cell growth, migration, and differentiation. Traditionally, the mechanisms and cues driving tumorigenesis, angiogenesis, and metastasis have been studied using either xenografts, which provide complex and convoluted microenvironments, or 2D culture systems, devoid of native biomechanical and biochemical cues.[1–3] The complexity of the in vivo cancer cell microenvironment in xenograft models makes it difficult to elucidate the role of individual components of the microenvironment on cell invasion. In contrast, the simplicity of traditional 2D culture systems, where cells are grown on hard polystyrene surfaces, makes it impossible to examine cell infiltration as a function of microenvironmental cues. 3D hydrogel models of the cancer cell microenvironment are needed to provide both a milieu of bioactive signals and a substrate that enables invasion.[4–7] While some breast cancer cell lines, such as the MDA-MB-231, are invasive, others, such as MCF-7 and T-47D cells, are not. A hydrogel that recapitulates the breast cancer microenvironment will support breast cancer cell invasive potential and maintain their morphology.

Several naturally derived and synthetic matrices have been studied. One of the most commonly studied ECM–mimetic materials, Matrigel, is derived from a mouse sarcoma and is consequently highly variable in composition and poorly defined. This reduces experimental reproducibility and makes the role of the ECM in cancer cell invasion and progression difficult to define. Collagen, another commonly used natural material, is intrinsically bioactive, however mechanical and chemical properties are fully coupled. The viscoelastic properties are manipulated by altering material concentration, which then inherently changes the density of endogenous signals. Synthetic materials, such as poly(ethylene glycol) (PEG)-based hydrogels, provide defined ECM analogs, yet are nonadhesive to cells, requiring additional signals to be incorporated therein.

S. A. Fisher, P. N. Anandakumaran, Prof. S. C. Owen, Prof. M. S. Shoichet
The Donnelly Centre for Cellular and Biomolecular Research
160 College Street, Room 514, Toronto, ON M5S 3E1, Canada
S. A. Fisher, Prof. S. C. Owen, Prof. M. S. Shoichet
Department of Chemical Engineering and Applied Chemistry
160 College Street, Room 514, Toronto, ON M5S 3E1, Canada
S. A. Fisher, P. N. Anandakumaran, Prof. S. C. Owen, Prof. M. S. Shoichet
Institute of Biomaterials and Biomedical Engineering
160 College Street, Room 514, Toronto, ON M5S 3E1, Canada
Prof. M. S. Shoichet
Department of Chemistry
University of Toronto
160 College Street, Room 514, Toronto, ON M5S 3E1, Canada
E-mail: molly.shoichet@utoronto.ca

DOI: 10.1002/adfm.201502778

The immobilization of bioactive molecules and adhesive ligands (i.e., RGDS) to PEG-based hydrogels have enabled controlled presentation of biological signals independently from material composition, supporting cell growth, differentiation, and migration.[8–11]

A hybrid hydrogel that combines a natural polymer backbone with engineered ECM mimetic crosslinks takes advantage of the bioactivity of natural polymers and the design component of synthetic polymers, thereby providing a defined microenvironment containing cell signaling sites and fully decoupled mechanical and chemical properties. Hyaluronic acid (HA) is overexpressed in tumor microenvironments and its accumulation around tumors has been correlated with poor patient outcomes and enhanced invasion of cancer cells.[12–15] The role of HA in cancer invasion, combined with its ease of chemical manipulation, makes it an ideal material with which to study cancer cell invasion.

We propose a tunable platform with which to study cancer cell invasion by independently manipulating crosslink and ligand densities. The HA backbone is modified with furan functionalities to enable hydrogel formation with bismaleimide peptide crosslinkers via a single-step Diels–Alder click reaction between the furan and maleimide groups (**Figure 1**A). HA–furan hydrogels crosslinked with bismaleimide PEG are degradable via hyaluronidase and support the attachment and proliferation of MDA-MB-231 cells, demonstrating the

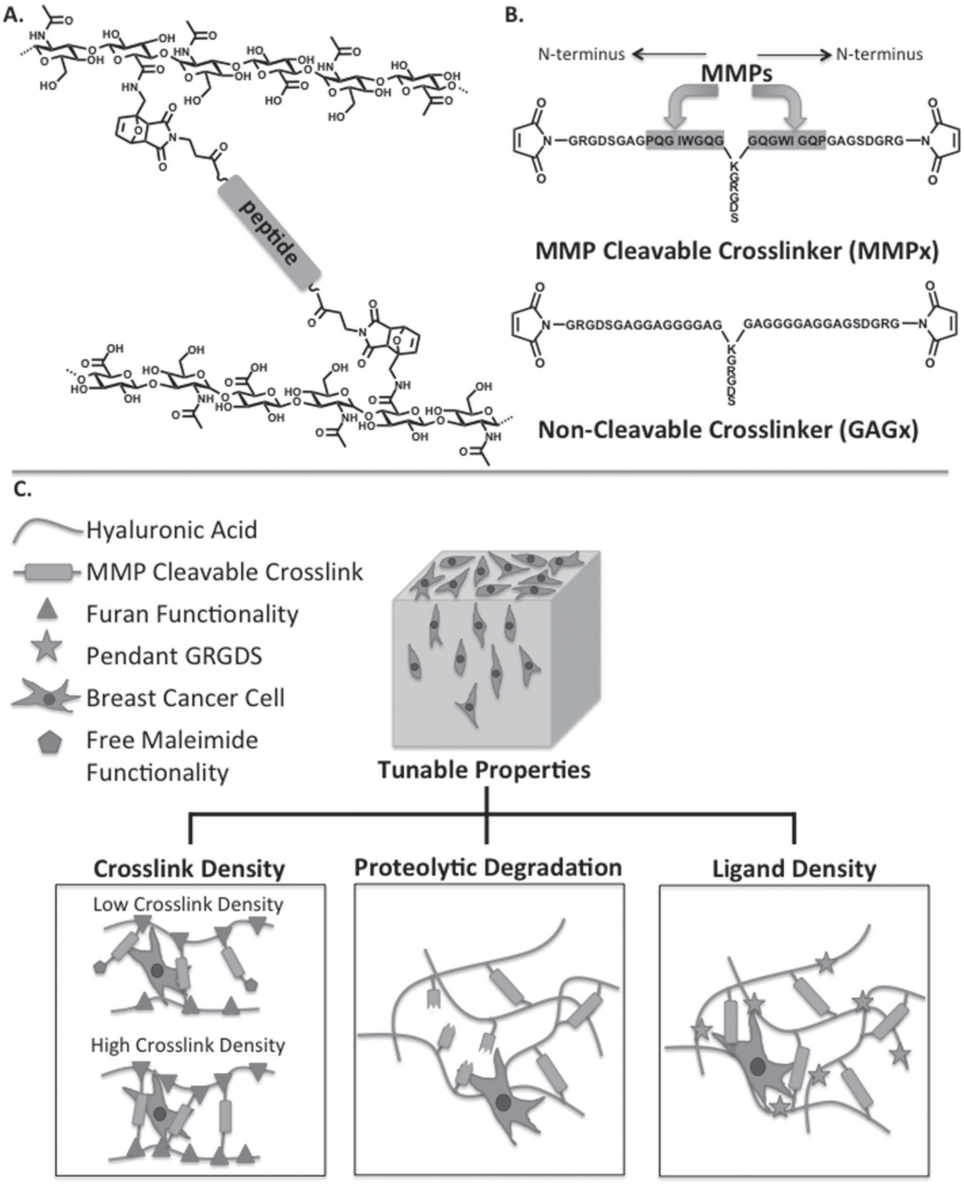

Figure 1. A) Bismaleimide peptide crosslinkers containing either an MMP-cleavable sequence (MMPx) or a noncleavable sequence (GAGx). The MMP susceptible sequence is highlighted with a rectangle. B) The furan-modified HA backbone is crosslinked with bismaleimide peptide crosslinkers (MMPx or GAGx) via Diels–Alder click chemistry to form HA hydrogels. C) Schematic diagram depicting modifications to the HA hydrogel, including tunable crosslink density, selective enzymatic degradation, and ligand density.

preservation of HA bioactivity following functionalization.[16] Crosslink density is controlled by the extent of furan modification on the HA backbone, thereby decoupling crosslink density from HA concentration.[17] Using a peptide crosslinker that is sensitive to cell-secreted proteases (GPQG↓IWGQ), the role of the matrix on cell invasion is further explored in the context of matrix metalloproteinase expression. This protease sensitive sequence can be cleaved by matrix metalloproteinases (MMP) 1, 2, 3, 7, 8, and 9, as previously shown.[18,19] Both the MMP cleavable crosslinker (MMPx) and noncleavable crosslinker (GAGx) contain three GRGDS sequences per crosslinker in addition to either two MMP cleavable or noncleavable sequences, respectively (Figure 1B). Thus, to decouple crosslink and ligand (GRGDS) densities, the quantity of crosslinker was maintained while either altering furan substitution or immobilizing additional pendant GRGDS. This new HA-peptide crosslink system is chemically defined and tunable. We eliminated the use of PEG, which was used in previous HA-crosslinked gels[16] and requires adhesive ligands for cell adhesion,[20] and replaced cysteine-terminated peptides, which can oxidize in air to form disulfide bridges, with maleimide-terminated peptides for Diels–Alder coupling with HA–furan.

To further tune the bioactivity of the HA hydrogels, noncrosslinking pendant ligands can be tethered onto the HA backbone using the same Diels–Alder click chemistry. The furan functionality on HA provides a customizable template to which a number of bioactive peptide sequences can be coupled, allowing the hydrogel to be further tailored to a desired microenvironment. A pendant maleimide-GRGDS (mal-GRGDS) was immobilized to the HA hydrogels to manipulate ligand density without changing viscoelastic properties, further tuning the hydrogel microenvironment for enhanced cell–matrix interactions.

In this study, we demonstrate the tunability of this ECM mimetic hydrogel as a platform to study breast cancer cell invasion. By independently varying mechanical and chemical properties, we gain insight into the importance of each of these factors to cell invasion (Figure 1C).

2. Results

2.1. Evaluation of Cancer Cell Invasion into HA Hydrogels

The HA/MMPx hydrogels were tested for cell invasion with a series of cancer cell lines that are either invasive (MDA-MB-231) or poorly invasive (MCF-7, SK-MEL-28, and T-47D). Each cell type was seeded on top of HA/MMPx hydrogels with medium crosslink density (1.25%, w/v HA, 40% furan substitution). After 4 d, cells were stained with DAPI and phalloidin and their depth of invasion was measured (**Figure 2**). The MCF-7, T-47D, and SK-MEL-28 remained on the gel surface, while the

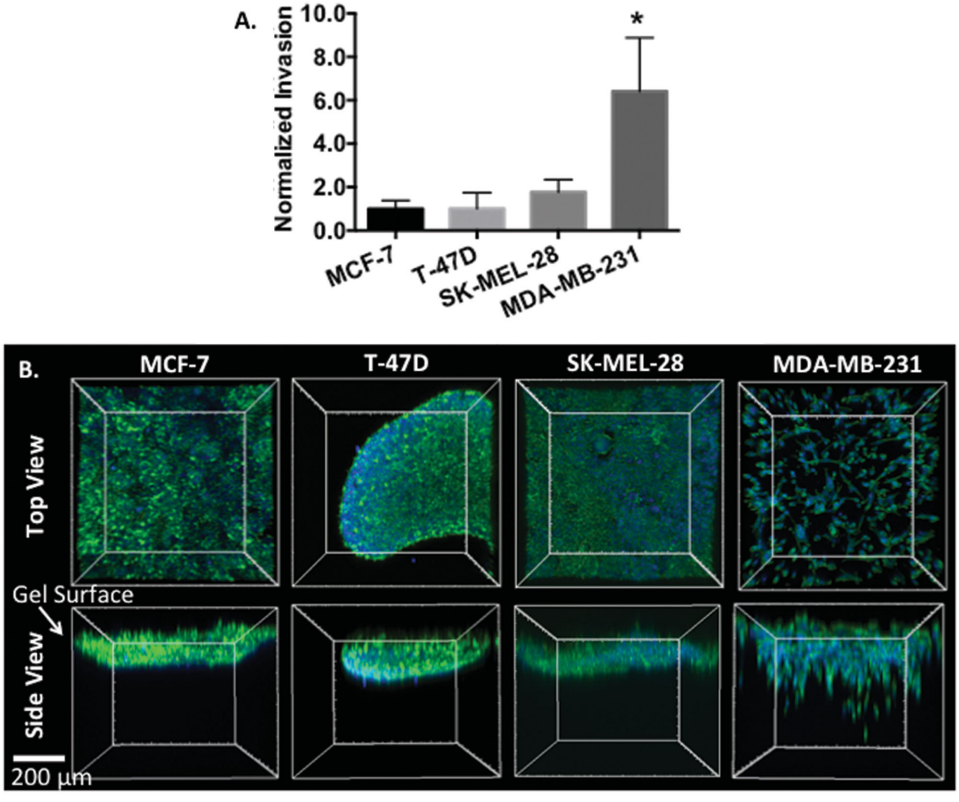

Figure 2. A) Quantification of cell invasion of MCF-7, T-47D, SK-MEL-28, and MDA-MB-231 into medium crosslink density HA/MMPx hydrogels at day 4 (mean + standard deviation, $n = 3$ independent studies, $*p < 0.05$). Invasion was normalized to the MCF-7s. B) Representative images of cells cultured on HA/MMPx hydrogels: 3D reconstruction of z-stack images (Imaris Bitplane). Cells stained with DAPI (blue) and phalloidin (green). MDA-MB-231 cells invaded into HA/MMPx while MCF-7, SK-MEL-28, and T-47D remained on the gel surface.

MDA-MB-231 cells readily infiltrated the HA/MMPx hydrogels. MCF-7 and T-47D cell lines are both noninvasive luminal breast cancer cells with epithelial morphology. When cultured on the HA/MMPx hydrogels they maintained a typical morphology: the MCF-7 cells formed a monolayer with a cobblestone appearance while the T-47D cells grew as adherent spheroids or clusters on the gel surface. To gain greater perspective on cell invasion, the SK-MEL-28 cell line, a malignant melanoma cell line with low/intermediate invasion potential,[21] was tested; however, SK-MEL-28 cells also failed to invade into medium crosslink density HA/MMPx, underlining the effect of mechanical properties on cell invasion even of a low/intermediate invasive cell line. In order to better understand how cell invasion would be affected by hydrogel properties, each of crosslink density and adhesive ligand density were independently tuned and studied in terms of MDA-MB-231 cell invasion.

2.2. Hydrogel Properties Influence Cell Invasion and Proliferation

2.2.1. Effect of Crosslink Density

To decouple the crosslink density from the ligand density, HA/MMPx hydrogels were formed with varying degrees of furan-substituted HA. Higher furan substitution increased the crosslink density and consequently the mechanical properties. The HA backbone was modified with 32%, 40%, and 55% furan, resulting in HA/MMPx hydrogels with low, medium, and high crosslink density, respectively. The concentration of MMPx remained constant between hydrogel formulations; the low and medium crosslinked gels had more MMPx with free ends than the high crosslinked density hydrogels. This ensured that the density of adhesive ligand binding sites also remained unchanged. The mechanical properties of the HA/MMPx hydrogels with low, medium, and high crosslink density were measured by compression testing. The Young's modulus was calculated for HA/MMPx hydrogels and was found to increase with higher furan substitution, as shown in **Figure 3**A. While not surprising that increased crosslink density would result in stiffer hydrogels, it is worth noting that the mechanical properties were manipulated independently from hydrogel composition—that is HA and MMPx concentrations were constant in the three hydrogels, with only furan substitution changing. Rheologic studies also revealed a correlation in gelation time with crosslink density: as crosslink density increased, gelation time significantly decreased, with gelation times of 106 ± 9, 87 ± 8, and 68 ± 10 min for low, medium, and high crosslink density gels, respectively (Figure 3B). This is likely due to the higher abundance of furan groups on the HA backbone, which increases the probability of reactions with the bis-maleimide crosslinkers, leading to faster gelation of the hydrogel.

After 4 d of culture, the MDA-MB-231 cells invaded significantly further into low crosslink density hydrogels than medium or high crosslink density hydrogels, with cells invading an average distance of 758 ± 78, 288 ± 78, and 85 ± 62 μm for low, medium, and high crosslink density gels, respectively (**Figure 4**A). Interestingly, there was no significant difference in cell number between any of the hydrogels, indicating that the cells interacted similarly with all of the hydrogels and the increased depth of invasion in the low crosslink density HA/MMPx hydrogels is not due to changes in cell number (Figure 4B). The 3D reconstructed images, from which the data in Figure 4A,B were derived, are shown in Figure 4C where the difference in depth of cell invasion in the three hydrogels is evident. A monolayer of MDA-MB-231 cells was present on the top of the high crosslink density gels with few cells penetrating and invading into the bulk matrix.

2.2.2. Effect of MMP Cleavable Hydrogels

In order to better understand the role of the MMP degradable crosslinker in the invasion of MDA-MB-231 cells, HA hydrogels crosslinked with MMPx were compared to those crosslinked with GAGx—a noncleavable peptide crosslinker.

To confirm that HA/MMPx hydrogels were cleavable, HA/GAGx and HA/MMPx were treated with collagenase type IV, and their change in mass was measured as a function of time. HA/MMPx hydrogels selectively degraded in the presence of 0.5 mg mL^{-1} collagenase type IV and were completely degraded after 36 h, while control HA/GAGx hydrogels had little change in mass, as shown in **Figure 5**A. Neither HA/MMPx nor HA/GAGx degraded in the presence of the HBSS buffer alone. This confirms that HA/GAGx hydrogels do not degrade in response to proteolytic degradation by MMPs, supporting the results that the enhanced invasion of MDA-MB-231 cells in HA/MMPx resulted from matrix degradation via cell-secreted MMPs.

To test the role of the MMP-cleavable crosslinker on cell invasion, MDA-MB-231 cells were cultured on the HA/MMPx and compared to those cultured on HA/GAGx. MDA-MB-231 cells invaded twice as far into HA/MMPx (278 ± 139 μm) than HA/GAGx (140 ± 61 μm) hydrogels after 4 d of culture, as shown in Figure 5B indicating that the invasion of MDA-MB-231 cells through the HA hydrogel is enhanced with the use

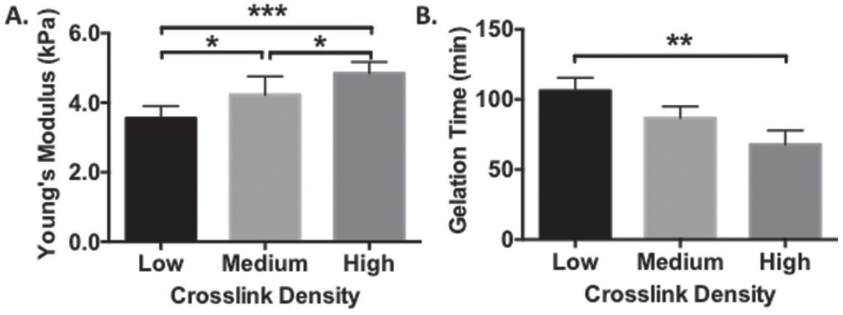

Figure 3. A) Young's moduli of HA/MMPx hydrogels with low, medium, and high crosslink density (mean + standard deviation, $n \geq 5$, $^{*}p < 0.05$, $^{***}p < 0.001$). B) Gelation time of HA/MMPx hydrogels with low, medium, and high crosslink density (mean + standard deviation, $n = 3$, $^{**}p < 0.01$).

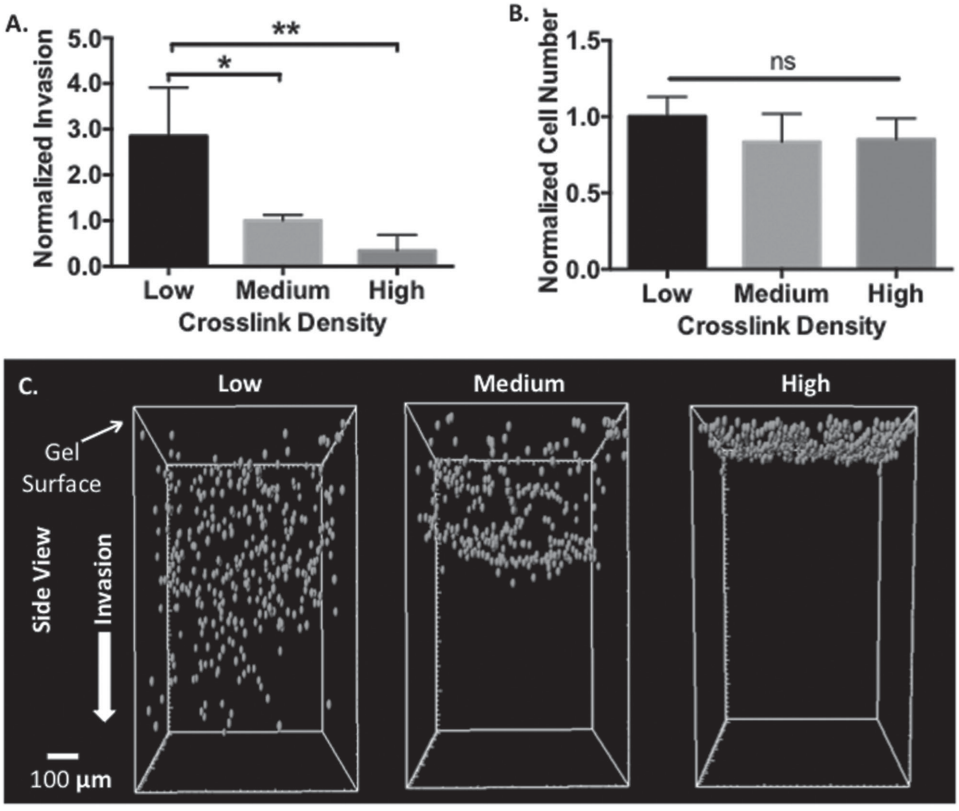

Figure 4. A) Quantification of MDA-MB-231 invasion into HA/MMPx hydrogels with low, medium, and high crosslink density at day 4, (mean + standard deviation, $n = 3$, $^{**}p < 0.01$). Invasion was normalized to medium crosslink density HA/MMPx. B) Normalized cell number of MDA-MB-231 cells in low, medium, and high crosslink density HA/MMPx at day 4 (mean + standard deviation, $n = 3$). Cell number was normalized to low crosslink density HA/MMPx and found to be unchanged among the groups. C) 3D reconstructions of z-stack images (Imaris Bitplane). Locations of cell nuclei are marked with ovals for visualization.

of crosslinkers susceptible to cleavage by MMPs. Importantly, there was no significant difference in cell number between HA/MMPx and HA/GAGx indicating that the increased invasion was not a result of increased proliferation (Figure 5C). The data quantified in Figure 5B and C were derived from images such as those shown in Figure 5D where cell invasion is significantly greater in MMPx-crosslinked gels.

Interestingly, even though the Young's modulus of HA/GAGx was found to be half that of HA/MMPx (S1, Supporting Information), there was still greater invasion into HA/MMPx. A molar equivalence of MMPx and GAGx was used to crosslink HA in each of HA/MMPx and HA/GAGx, yet since the molar mass of GAGx (3205.12 g mol^{-1}) is less than that of MMPx (3883.99 g mol^{-1}), the mass/volume of GAGx was lower, which may explain the lower modulus of HA/GAGx. While data in Figure 4 showed greater cell invasion in softer gels, this was not replicated here due to the use of a nondegradable linker. This suggests that the MDA-MB-231 cells are actively degrading the matrix as they are migrating through HA/MMPx.

To gain greater insight into the mechanism of cell invasion into the MMPx crosslinked hydrogels, MDA-MB-231 cells were cultured on HA/MMPx hydrogels in the presence of a broad-spectrum MMP inhibitor, GM6001. Here, we observed reduced MDA-MB-231 invasion into HA/MMPx gels in the presence of GM6001, thereby demonstrating MMP-mediated degradation (**Figure 6**A). Importantly, the presence of GM6001 did not have a significant effect on the number of cells growing on the HA/MMPx hydrogels containing either no (i.e., 0) or 25×10^{-6} M GM6001 (Figure 6B).

2.2.3. Effect of GRGDS Ligand Density

To determine the influence of tuning the adhesive ligand density independently from hydrogel mechanics on MDA-MB-231 cell invasion, pendant mal-GRGDS groups were immobilized into medium crosslink density HA/MMPx hydrogels. To demonstrate that mal-GRGDS (641.60 g mol^{-1}) was able to diffuse and immobilize into HA/MMPx, a model molecule (Alexa-Fluor546-maleimide, 1034.37 g mol^{-1}) was immobilized using the same method, and shown to be distributed throughout the hydrogel (S2, Supporting Information). There were no significant differences in the invasion of MDA-MB-231 cells after 4 d of culture in HA/MMPx with 0×10^{-6}, 493×10^{-6}, or 1327×10^{-6} M additional mal-GRGDS with cells invading an average distance of 284 ± 72, 377 ± 44, and 352 ± 16 µm, respectively (**Figure 7**A). However, the HA/MMPx with the highest ligand density (1327×10^{-6} M) had significantly (1.6 times) more cells than HA/MMPx with no additional mal-GRGDS (0×10^{-6} M), as shown in Figure 7B quantitatively and

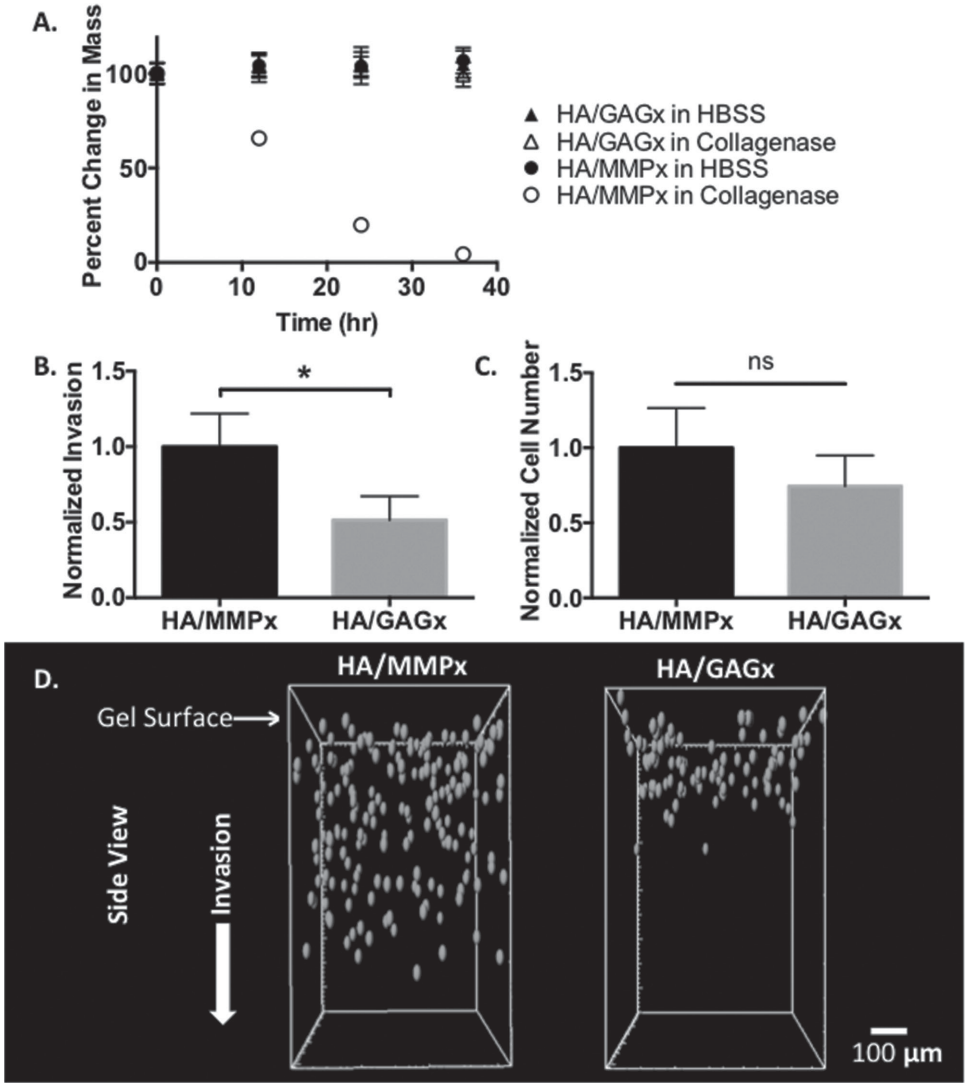

Figure 5. A) Percent change in mass of HA/GAGx and HA/MMPx in HBSS buffer or HBSS buffer with 0.5 mg mL^{-1} collagenase type IV. Only HA/MMPx selectively degraded in collagenase type IV (mean ± standard deviation, $n = 3$). B) Quantification of MDA-MB-231 cell invasion into medium crosslink density HA/MMPx and HA/GAGx hydrogels at day 4 (mean + standard deviation, $n = 3$, $^*p < 0.05$). Invasion into HA/GAGx was normalized to HA/MMPx. C) Normalized cell number of MDA-MB-231 cells in HA/MMPx and HA/GAGx at day 4 (mean + standard deviation, $n = 3$). MDA-MB-231 cell number in HA/GAGx was normalized to HA/MMPx. D) Imaris Bitplane 3D reconstructions of z-stack images. Locations of cell nuclei are marked with ovals for visualization.

in Figure 7C with representative images. This demonstrates the proliferative effect of GRGDS on MDA-MB-231 cells.

3. Discussion

Intrinsic mechanical properties of the microenvironment play a critical role in cell growth, differentiation, and migration, directing tissue development, and maintaining homeostasis.[22] During tumorigenesis, the stiffness of the local ECM increases,[23–25] and cells have been shown to adapt to this increase in ECM stiffness by strengthening focal adhesions through Rho-mediated actomyosin contraction.[26,27] This leads to higher traction and protrusion forces to enable cellular infiltration into a denser medium.[28–30] Collagen crosslinking and ECM stiffening have also been reported in breast cancer, promoting an increase in focal adhesions, PI3 kinase activity, and invasion.[25] The Young's Modulus of normal breast fat and fibroglandular tissue has been reported to be approximately 3 kPa, matching the stiffness of the 1.25% medium crosslink density HA/MMPx used in this study (S3, Supporting Information).[24] Therefore, HA/MMPx can mimic the mechanical environment encountered by breast cancer cells once they leave the primary tumor and invade into the surrounding ECM.

Low and medium crosslink density HA/MMPx readily allowed MDA-MB-231 invasion, with medium crosslink density gels showing greater resistance to the invading cells. MDA-MB-231 cells showed minimal invasion into the high crosslink density HA/MMPx. While the higher crosslink density hydrogel has a higher modulus, it also has more crosslinking groups that have

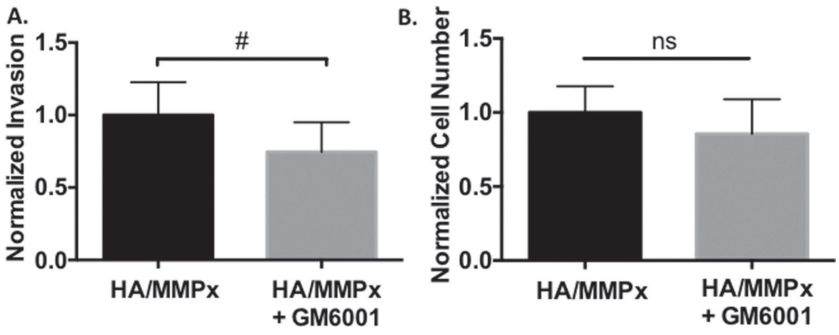

Figure 6. A) Quantification of MDA-MB-231 cell invasion into medium crosslink density HA/MMPx hydrogels with or without GM6001 MMP inhibitor at day 3 (mean + standard deviation, $n = 5$, $\#p < 0.10$). MDA-MB-231 invasion into HA/MMPx with GM6001 (25×10^{-6} M) was normalized to HA/MMPx without GM6001 (0×10^{-6} M). The GM6001 inhibitor reduces cell invasion. B) Normalized cell number of MDA-MB-231 cells in medium crosslink density HA/MMPx with (25×10^{-6} M) or without (0×10^{-6} M) GM6001 MMP inhibitor at day 3 (mean + standard deviation, $n = 5$). MDA-MB-231 cell number in HA/MMPx with GM6001 was normalized to HA/MMPx without GM6001 and was found to be unchanged.

to be cleaved to allow cell invasion. The need for more localized matrix degradation hindered the invasion of MDA-MB-231 cells, and resulted in minimal infiltration into the high crosslink density HA/MMPx hydrogels after 4 d of culture. With fewer MMP cleavable sequences needing to be cleaved in low vs. high crosslink density gels, the invasion into the low crosslink density HA/MMPx is therefore less dependent on MMP-mediated degradation. The Burdick group has developed an HA-based hydrogel that gels via Michael addition between maleimide-functionalized HA and cysteine containing peptide crosslinkers. They found that when the crosslink density was increased with greater maleimide substitution on the HA backbone, the rate of degradation with collagenase type II decreased, supporting our hypothesis that in high crosslink density gels more crosslinks need to be cleaved in order to allow cell invasion.[31] A stiffer, denser matrix has also been shown to hinder cell invasion by slowing the velocity of migrating cells.[10] The speed of migrating cells increases with increasing pore size when pores are the same size scale or slightly smaller than the migrating cell body.[32] At larger pore sizes, cellular velocity decreases as cells lose the matrix connections needed to gain traction.[33] The pore size of the low, medium, and high crosslink density HA/MMPx used in

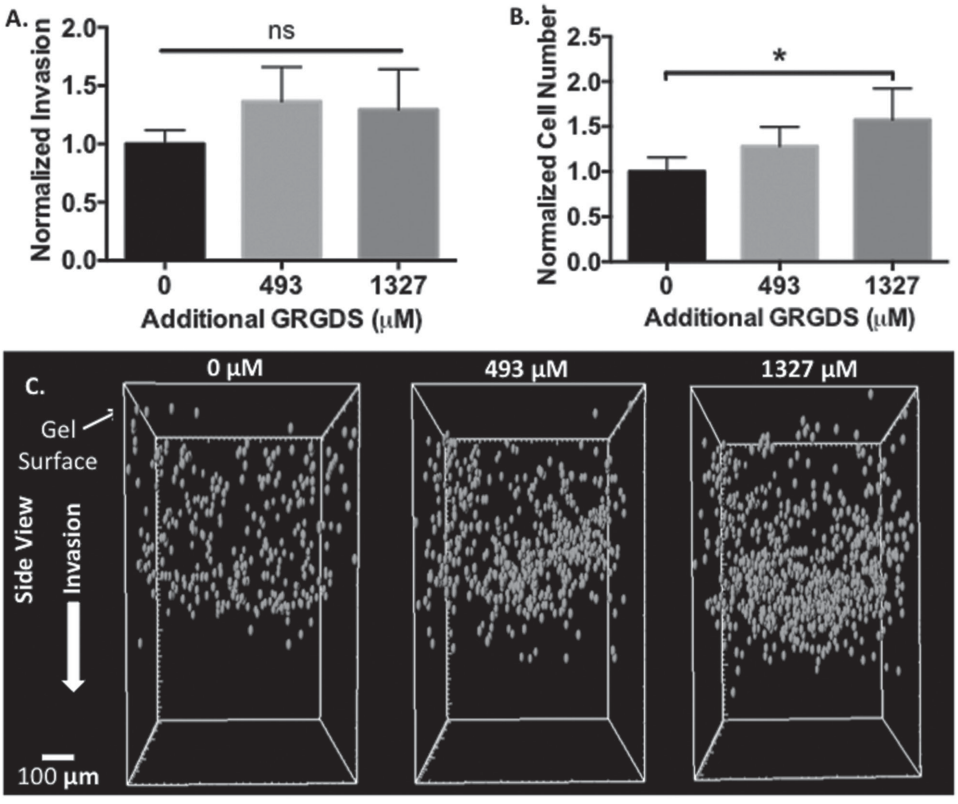

Figure 7. A) Quantification of invasion of MDA-MB-231 cells into medium crosslink density HA/MMPx hydrogels containing 0×10^{-6}, 493×10^{-6}, or 1327×10^{-6} M of additional pendant GRGDS on day 4 (mean + standard deviation, $n = 4$). Invasion was normalized to HA/MMPx with no additional mal-GRGDS. B) Normalized MDA-MB-231 cell number in medium crosslink density HA/MMPx hydrogels containing 0×10^{-6}, 493×10^{-6}, or 1327×10^{-6} M additional mal-GRGDS on day 4 (mean + standard deviation, $n = 4$, $*p < 0.05$). Cell number was normalized to HA/MMPx with 0×10^{-6} M additional mal-GRGDS to facilitate comparison between independent studies. C) Imaris Bitplane 3D reconstructions of z-stack images. Locations of cell nuclei are marked with ovals for visualization.

this study was estimated to be 16.5 ± 1.2, 15.5 ± 0.7, 14.7 ± 0.8 nm, respectively (S4, Supporting Information). The pore sizes of HA/MMPx are within the range typically found in hydrogels (5 nm up to several μm),[32,34,35] and similar to the 20–130 nm pore sizes found in tumor ECM.[36]

The interplay between matrix mechanics and cell-mediated degradation will dictate the speed and mechanism of cellular movement through hydrogels in vitro, and these properties must be fully tunable to recapitulate a full range of tissue properties. To migrate through the ECM, cells must either squeeze through existing pores in the matrix or use proteolytic strategies to locally degrade ECM around the cell body. Cancer cells have been reported to overexpress proteases including MMPs 1, 2, 7, 9, 13, and 14, which increase their invasiveness through tissue and are associated with poor patient prognosis.[37–42] Collagenase type IV, which includes MMPs 2 and 9, was shown to degrade HA/MMPx, supporting the use of the MMP cleavable sequence GPQG↓IWGQ to enhance cancer cell invasion. MDA-MB-231 cells were shown to invade twice as far into MMP cleavable hydrogels (HA/MMPx) compared with noncleavable HA hydrogels (HA/GAGx), despite HA/GAGx having half the stiffness of HA/MMPx. The mechanism of invasion was further confirmed by culturing MDA-MB-231 cells on HA/MMPx hydrogels treated with or without the small molecule MMP inhibitor GM6001. GM6001 contains a hydroxamic group that chelates zinc from the catalytic domain of MMPs, resulting in a reversible inhibition of protease activity.[43,44] We acknowledge that some MMP-independent cell invasion occurred as some MDA-MB-231 cells migrated into both the HA/GAGx hydrogels and HA/MMPx hydrogels containing GM6001. This may be attributed to hyaluronidase-mediated degradation, an enzyme known to be secreted by MDA-MB-231 cells.[16,45] When pores are similar sizes as cells, cells may be able to push the matrix network apart or rearrange their cytoskeleton to pass through the existing pores.[46,47] However, because the estimated pore size of HA/MMPx is much smaller than a cell body, the MMP independent invasion in our hydrogels is likely due to hyaluronidase-mediated degradation. GM6001 has been shown to have minimal impact on cell invasion into matrices where cells can convert between MMP-dependent and independent invasion mechanisms.[47,48]

To gain greater insight in the cell–matrix interactions, the hydrogel microenvironment was modified with adhesive ligands. Cell adhesion to the ECM is mediated predominantly through the binding of integrins to adhesive proteins in the matrix. This initiates downstream signaling pathways, which regulate cell proliferation, motility, and differentiation.[49] NIH-3T3 fibroblast attachment, spreading, and proliferation increased on polystyrene surfaces modified with increasing density of the cell adhesive GRGDSY peptide.[50] Similarly, the growth rate of MC3T3 preosteoblasts cultured on alginate hydrogels correlated with the concentration of covalently bound GGGGRGDSP; a maximum growth rate was observed at 3570 RGD μm^{-2}, beyond which cell growth decreased with increasing GGGGRGDSP concentrations.[51] In our HA hydrogels, the number of MDA-MB-231 cells within the HA/MMPx hydrogels increased with higher GRGDS concentrations; however, the depth of invasion was not significantly different. This suggests that the peptide ligand density has a greater effect on proliferation than migration at the GRGDS concentrations tested, consistent with literature. Lutolf et al. found an increase in the invasion rate of human foreskin fibroblasts in MMP cleavable PEG based hydrogels with increasing RGDSP concentrations, from 10×10^{-6} to 42.5×10^{-6} M.[19] However, these are lower than the concentrations that can be achieved in our hydrogels due to an inherent GRGDS concentration present in the MMPx and GAGx crosslinkers. At higher RGDSP concentrations (140×10^{-6} to 340×10^{-6} M), Lutolf et al. observed no effect on cell invasion, consistent with our observations.[19]

4. Conclusions

The current study demonstrates the importance of tunability in ECM mimetic HA hydrogels and the corresponding impact on the invasion and proliferation of MDA-MB-231 breast cancer cells. Decoupling crosslink and adhesive ligand densities is crucial to engineering hydrogels that recapitulate a wide variety of microenvironments. We demonstrate that cell invasion is mediated by an MMP mechanism, reduced with stiffer (high crosslink density) gels, and unaffected by adhesive ligand concentration. In softer HA/GAGx hydrogels cell invasion is reduced relative to that observed in HA/MMPx, underlining the importance of cell-mediated degradation to invasion. The tunability of the HA/MMPx hydrogels allows independent manipulation and investigation of mechanical, chemical, and biological cues. HA/MMPx hydrogels provide a platform to study breast cancer cell invasion and the cues that drive it. By controlling the mechanical and chemical environment of ECM mimetic hydrogels, our understanding of the role of the microenvironment on cell invasion is enhanced.

5. Experimental Section

Materials: Lyophilized sodium hyaluronate (HA) was purchased from Lifecore Biomedical (2.15×10^5 amu) (Chaska, MN, USA). Collagenase type IV, 4-(4,6-dimethoxy-1,3,5-triazin-2-yl)-4-methylmorpholinium chloride (DMTMM), *N,N′*-diisopropylcarbodiimide (DIC), triisopropyl silane (TIS), furfurylamine, and Dulbecco's phosphate buffered saline (PBS) were purchased from Sigma–Aldrich (St. Louis, MO, USA). Sodium chloride and 2-(*N*-morpholino)ethanesulfonic acid (MES) were purchased from BioShop Canada Inc. (Burlington, ON, Canada). Trifluoroacetic acid (TFA) and all solvents were purchased from Caledon Laboratory Chemicals (Georgetown, ON, Canada). Fmoc-protected amino acids and Wang resin were purchased from AnaSpec (Fremont, CA, USA). 3-Maleimidopropionic acid was purchased Toronto Research Chemicals (Toronto, ON, Canada). Dialysis membranes were purchased from Spectrum Laboratories (Rancho Dominguez, CA, USA). Eight-well chamber slides (Nunc) were purchased from Thermo Scientific (Waltham, MA USA). GM6001 MMP inhibitor was purchased from EMD Millipore (Billerica, MA, USA). Hank's Buffered Salt Solution (HBSS) and cell culture media were purchased from Life Technologies (Carlsbad, CA, USA). Distilled deionized water (ddH_2O) was prepared using a Millipore Milli-RO 10 Plus and Milli-Q UF Plus at 18 MΩ resistance (Millipore, Bedford, MA, USA).

Synthesis of Maleimide-Functionalized Peptides: Peptides were synthesized using standard Fmoc chemistry on a Liberty 1 peptide synthesizer equipped with a Discover microwave reactor (CEM, Matthews, NC, USA). Following final deprotection of the N-terminus, maleimide functionalities were added to the peptide by coupling 3-maleimidopropionic acid to the free amines with DIC. Peptides were

then cleaved from the resin with a solution of 80% TFA, 10% dH_2O, and 10% TIS, precipitated with ice-cold ethyl ether, and purified via high-performance liquid chromatography (HPLC). Two peptide crosslinkers were synthesized: an MMP cleavable crosslinker (MMPx) and a noncleavable crosslinker (GAGx). The GAGx crosslinker was designed to have the same number of amino acids as MMPx, the same pI of 10.08 and the same net charge of +1 at pH 7 (for the linear sequence). Additionally, since GAG is often used as a spacer sequence in peptides due to its lack of bioactivity, GAGx was a useful, nonactive control peptide crosslinker.

Synthesis of HA Hydrogels: Furan-modified HA (HA–furan) was synthesized as previously described.[16] Briefly, HA–furan was synthesized by dissolving HA in MES (pH 5.5, 100×10^{-3} M) to achieve a concentration of 1.00% w/v HA. DMTMM was added followed by the dropwise addition of furfurylamine. The molar equivalences of DMTMM and furfurylamine were varied to achieve the desired furan substitutions of 32%, 40%, and 55%.[16,17] The reaction was stirred at room temperature for 24 h and dialyzed (12–14 kDa MWCO) against 0.1 M NaCl for 2 d followed by ddH_2O for 2 d. Furan substitution was confirmed via ^1H NMR in D_2O on an Agilent DD2-500 MHz NMR spectrometer (Santa Clara, CA, USA). The ratio of the area under the furan proton peaks (6.26, 6.46, and 7.65 ppm) to the area under the peak for *N*-acetyl glucosamine protons on HA (1.9 ppm) determined the degree of furan substitution.

To form the hydrogels, HA–furan and the bis-maleimide peptide crosslinker were separately dissolved in equal volumes of MES buffer (pH 5.5, 100×10^{-3} M). The crosslinker concentration was maintained between all formulations, with the molar equivalence of furan:maleimide being 0.8:1, 1:1, 1.4:1 for HA hydrogels made with 32, 40, and 55% furan-substituted HA, respectively. The HA–furan and bis-maleimide peptide crosslinker solutions were thoroughly mixed together, filtered through a 0.22 µm syringe filter, and gelled overnight at 37 °C to form the HA hydrogels. Hydrogels were washed with PBS followed by cell culture media to condition the hydrogels and raise the pH to 7.4. The reported hydrogel percent herein refers to the concentration of HA used in each formulation.

Mechanical Compression Testing: The Young's moduli of the HA hydrogels were measured using cylindrical samples with a diameter of 5 mm. The hydrogels were placed between two impermeable platens connected to a DAQ-Nano17 force transducer (ATI Industrial Automation) attached to a Mach-1 micromechanical system (Biomomentum). An initial force of 0.01 N was applied to tare samples, and the platen-to-platen separation was taken as the initial sample height. Samples underwent uniaxial unconfined compression at 37 °C at a rate of 10 µm s^{-1} until an applied strain of 20% was reached. The Young's modulus was determined from the resultant stress–strain curve.

Rheology: The viscoelastic properties of the HA/MMPx hydrogels were determined using an AR-1000 rheometer fitted with a 20 mm, 1° acrylic cone using parallel plate geometry and a solvent trap to reduce evaporation (TA Instruments, New Castle, DE, USA). The hydrogel solutions were loaded onto the rheometer and the upper plate was lowered to a gap size of 20 µm. A time sweep was performed at 37 °C and 0.2% strain for 7.5 h to allow for complete gelation. The time at which G' (shear storage modulus) crossed G'' (shear loss modulus) was taken as the hydrogels gelation time. Following the time sweep, a strain sweep was conducted to ensure that the strain and frequency were within the linear viscoelastic region.

Degradation of MMP Cleavable Hydrogels: HA hydrogels were formed with either MMPx or GAGx (1.00% w/v HA, 100 µL volume) in preweighed tubes, washed in HBSS for 24 h, excess buffer was removed and the hydrogels were weighed to determine their initial mass. Then either HBSS (200 µL) or 0.5 mg mL^{-1} collagenase type IV in HBSS (200 µL) was added to the hydrogels. Every 12 h the excess supernatant was removed from the hydrogels, the hydrogels were weighed, and a fresh solution of HBSS with or without collagenase type IV was added. This was repeated until the HA/MMPx gels fully degraded in collagenase.

Quantification of Immobilized GRGDS: Only for the purposes of quantifying the amount of mal-GRGDS immobilized into the HA hydrogels, a model hydrogel system composed of PEG-crosslinked HA was used, as the high concentration of amino acids present in the MMPx-crosslinked HA hydrogels complicated this analysis. 1.25% w/v HA hydrogels were crosslinked with bis-maleimide-polyethylene glycol (PEG) crosslinkers and gelled overnight at 37 °C in eight-well chamber slides. Pendant mal-GRGDS (0, 0.84, or 1.67 mg) dissolved in MES buffer (150 µL, 100×10^{-3} M, pH 5.5) was added to each HA/PEG hydrogel and soaked overnight. The pendant mal-GRGDS reacted with furan functionalities on the HA backbone that remained following the crosslinking reaction. The unbound mal-GRGDS was then thoroughly washed out with PBS. The HA hydrogels were then dissolved by adding hyaluronidase (150 µL, 100 U mL^{-1}) in MES at 37 °C for 2 d until complete degradation occurred. The quantity of mal-GRGDS immobilized to the hydrogels was determined via amino acid analysis to be 0, $493 \pm 201 \times 10^{-6}$ M, $1327 \pm 247 \times 10^{-6}$ M. It is these values of pendant GRGDS, independent of the concentration of GRGDS in the MMPx crosslinker, to which we refer in studies of the effect of ligand concentration on cell invasion.

Maintenance of Cancer Cell Lines: Cell lines were maintained in tissue culture flasks in an incubator (37 °C, 5% CO_2, 95% humidity) using their corresponding growth medium: MDA-MB-231, T-47D and SK-MEL-28 in RPMI-1640, and MCF-7 in Dulbecco's modified Eagle's medium Nutrient Mixture F-12 Ham. All cell culture media were supplemented with 10% FBS, penicillin (10 U mL^{-1}), and streptomycin (10 µg mL^{-1}). T-47D and MCF-7 growth media were also supplemented with insulin (10 µg mL^{-1}). All cell lines were purchased from ATCC (Manassas, VA).

Quantification of Cancer Cell Invasion and Proliferation: After forming HA/(MMPx or GAGx) hydrogels (125 µL) in 8 well chamber slides, 2×10^4 cancer cells per well were seeded on the hydrogel surface on the following day. The cells were cultured on the hydrogels for 4 d before being fixed with 4% paraformaldehyde and stained with DAPI for visualization of cell nuclei. The hydrogels were imaged on an Olympus Fluoview FV1000 confocal microscope with *xy* scans every 5 µm in the *z*-direction. For quantification of invasion and cell number, each *z*-stack was divided into 4 quadrants, and the position coordinate of each nuclei was determined using Imaris Bitplane. The depth of invasion was calculated as the depth occupied by 80% of the cells. The top and bottom 10% of cells in each quadrant were discounted in order to minimize the effect of surface defects and/or single cells that had invaded great distances, skewing the results (S5, Supporting Information). The depth occupied by 80% of the cells in the four quadrants was averaged to obtain the depth of invasion for the *z*-stack. Cell number was quantified as the total number of nuclei within the *z*-stack.

To determine the effects of tuning the hydrogels' crosslink density, proteolytic degradation of the crosslinker, and ligand density on the invasion of MDA-MB-231 cells, the following hydrogel modifications were made: 1) To vary crosslink density, 1.25% w/v HA/MMPx hydrogels were formed from HA with varying furan substitutions (32%, 40%, and 55%) herein referred to as having low, medium, or high crosslink densities, respectively. To maintain a consistent ligand density, the amount of MMPx remained the same between low, medium, and high crosslink density hydrogels. 2) To determine the influence of proteolytic degradation of the peptide crosslinker on invasion, medium crosslink density, 1.00% w/v HA hydrogels were formed with either MMPx or GAGx. 3) To confirm the influence of MMP-dependent invasion, MDA-MB-231 cells were cultured on 1.25% w/v HA/MMPx with (25×10^{-6} M) or without (0×10^{-6} M) the MMP inhibitor GM6001. Both treatment groups contained 1% v/v DMSO in media. Hydrogels were preincubated in media containing 0×10^{-6} M or 25×10^{-6} M GM6001, and media were changed daily throughout the experiment. 4) To vary ligand density, prior to neutralizing HA/MMPx, pendant mal-GRGDS (0, 0.84, or 1.67 mg) was dissolved in MES buffer (150 µL, 100×10^{-3} M, pH 5.5) and soaked into medium crosslink density, 1.25% w/v HA/MMPx hydrogels overnight. After removing the mal-GRGDS supernatant, the hydrogels were washed thoroughly with PBS followed by cell culture media to remove unbound mal-GRGDS and neutralize the hydrogel.

Statistical Analysis: All statistical analyses were performed using GraphPad Prism version 6 (GraphPad Software, San Diego, CA, USA, www.graphpad.com). Differences among 3 or more groups were assessed using one-way ANOVA followed by Bonferonni post-hoc corrections to identify statistical significance. Differences between two groups were

assessed using an unpaired *t*-test. For all statistical analyses, α was set at 0.10. Data were displayed with *p* values represented as $\#p \leq 0.10$, $*p \leq 0.05$, $**p \leq 0.01$, $***p \leq 0.001$. No significance (ns) was indicated for $p > 0.10$. Each experiment was repeated a minimum of three times for accuracy.

Supporting Information

Supporting Information is available from the Wiley Online Library or from the author.

Acknowledgements

The authors thank Dr. Senthil Muthuswamy for helpful discussions and advice. The authors are grateful to the Natural Sciences and Engineering Research Council of Canada (NSERC) and the Canadian Institutes for Health Research (CIHR) for funding provided through the Collaborative Health Research Program. S.A.F. is grateful to NSERC for PGSD scholarship and P.N.A. is grateful to the NSERC CREATE in M3 for funding. The authors acknowledge the Canada Foundation for Innovation, project number 19119, and the Ontario Research Fund for funding of the Centre for Spectroscopic Investigation of Complex Organic Molecules and Polymers.

Received: July 7, 2015
Revised: September 15, 2015
Published online: November 2, 2015

[1] W. M. van Weerden, J. C. Romijn, *Prostate* **2000**, *43*, 263.
[2] V. Hongisto, S. Jernström, V. Fey, J. P. Mpindi, K. Kleivi Sahlberg, O. Kallioniemi, M. Perala, *PLoS One* **2013**, *8*, e77232.
[3] E. A. Sausville, A. M. Burger, O. J. Becher, E. C. Holland, *Cancer Res.* **2006**, *66*, 3351.
[4] K. L. Schmeichel, M. J. Bissell, *J. Cell Sci.* **2003**, *116*, 2377.
[5] F. Pampaloni, E. G. Reynaud, E. H. K. Stelzer, *Nat. Rev. Mol. Cell Biol.* **2007**, *8*, 839.
[6] M. H. Zaman, *Nat. Rev. Cancer* **2013**, *13*, 596.
[7] S. C. Owen, M. S. Shoichet, *J. Biomed. Mater. Res.* **2010**, *94*, 1321.
[8] D. S. W. Benoit, A. R. Durney, K. S. Anseth, *Biomaterials* **2007**, *28*, 66.
[9] J. E. Leslie-Barbick, J. E. Saik, D. J. Gould, M. E. Dickinson, J. L. West, *Biomaterials* **2011**, *32*, 5782.
[10] K. A. Kyburz, K. S. Anseth, *Acta Biomater.* **2013**, *9*, 6381.
[11] G. H. Underhill, A. A. Chen, D. R. Albrecht, S. N. Bhatia, *Biomaterials* **2007**, *28*, 256.
[12] M. A. Anttila, R. H. Tammi, M. I. Tammi, K. J. S. nen, S. V. Saarikoski, V.-M. Kosma, *Cancer Res.* **2000**, *60*, 150.
[13] N. Liu, F. Gao, Z. Han, X. Xu, C. B. Underhill, L. Zhang, *Cancer Res.* **2001**, *61*, 5207.
[14] B. P. Toole, C. Biswas, J. Gross, *Proc. Natl. Acad. Sci. USA* **1979**, *76*, 6299.
[15] B. Bernert, H. Porsch, P. Heldin, *J. Biol. Chem.* **2011**, *286*, 42349.
[16] C. M. Nimmo, S. C. Owen, M. S. Shoichet, *Biomacromolecules* **2011**, *12*, 824.
[17] S. C. Owen, S. A. Fisher, R. Y. Tam, C. M. Nimmo, M. S. Shoichet, *Langmuir* **2013**, *29*, 7393.
[18] H. Nagase, G. B. Fields, *Biopolymers* **1996**, *40*, 399.
[19] M. P. Lutolf, J. L. Lauer-Fields, H. G. Schmoekel, A. T. Metters, F. E. Weber, G. B. Fields, J. A. Hubbell, *Proc. Natl. Acad. Sci. USA* **2003**, *100*, 5413.
[20] H. Du, P. Chandaroy, S. W. Hui, *Biochim. Biophys. Acta, Biomembr.* **1997**, *1326*, 236.
[21] A. Klose, A. Wilbrand-Hennes, P. Zigrino, E. Weber, T. Krieg, C. Mauch, N. Hunzelmann, *Int. J. Cancer* **2006**, *118*, 2735.
[22] C. C. DuFort, M. J. Paszek, V. M. Weaver, *Nat. Rev. Mol. Cell Biol.* **2011**, *12*, 308.
[23] M. J. Paszek, V. M. Weaver, *J. Mammary Gland Biol. Neoplasia* **2004**, *9*, 325.
[24] A. Samani, J. Zubovits, D. Plewes, *Phys. Med. Biol.* **2007**, *52*, 1565.
[25] K. R. Levental, H. Yu, L. Kass, J. N. Lakins, M. Egeblad, J. T. Erler, S. F. T. Fong, K. Csiszar, A. Giaccia, W. Weninger, M. Yamauchi, D. L. Gasser, V. M. Weaver, *Cell* **2009**, *139*, 891.
[26] N. Q. Balaban, U. S. Schwarz, D. Riveline, P. Goichberg, G. Tzur, I. Sabanay, D. Mahalu, S. Safran, A. Bershadsky, L. Addadi, B. Geiger, *Nat. Cell Biol* **2001**, *3*, 466.
[27] B. Geiger, J. P. Spatz, A. D. Bershadsky, *Nat. Rev. Mol. Cell Biol.* **2009**, *10*, 21.
[28] H. J. Kong, T. R. Polte, E. Alsberg, D. J. Mooney, *Proc. Natl. Acad. Sci. USA* **2005**, *102*, 4300.
[29] S. I. Fraley, Y. Feng, R. Krishnamurthy, D.-H. Kim, A. Celedon, G. D. Longmore, D. Wirtz, *Nat. Cell Biol.* **2010**, *12*, 598.
[30] W. R. Legant, J. S. Miller, B. L. Blakely, D. M. Cohen, G. M. Genin, C. S. Chen, *Nat. Methods* **2010**, *7*, 969.
[31] J. L. Holloway, H. Ma, R. Rai, J. A. Burdick, *J. Controlled Release* **2014**, *191*, 63.
[32] G. P. Raeber, M. P. Lutolf, J. A. Hubbell, *Biophys. J.* **2005**, *89*, 1374.
[33] B. A. C. Harley, H.-D. Kim, M. H. Zaman, I. V. Yannas, D. A. Lauffenburger, L. J. Gibson, *Biophys. J.* **2008**, *95*, 4013.
[34] S. Kirchhof, M. Abrami, V. Messmann, N. Hammer, A. M. Goepferich, M. Grassi, F. P. Brandl, *Mol. Pharm.* **2015**, *12*, 3358.
[35] J. B. Leach, K. A. Bivens, C. W. Patrick Jr., C. E. Schmidt, *Biotechnol. Bioeng.* **2003**, *82*, 578.
[36] A. Pluen, Y. Boucher, S. Ramanujan, T. D. McKee, T. Gohongi, E. di Tomaso, E. B. Brown, Y. Izumi, R. B. Campbell, D. A. Berk, R. K. Jain, *Proc. Natl. Acad. Sci. USA* **2001**, *98*, 4628.
[37] O. C. Kousidou, A. E. Roussidis, A. D. Theocharis, N. K. Karamanos, *Anticancer Res.* **2004**, *24*, 4025.
[38] M. Périgny, I. Bairati, I. Harvey, M. Beauchemin, F. Harel, M. Plante, B. Têtu, *Am. J. Clin. Pathol.* **2008**, *129*, 226.
[39] T. Yamada, T. Oshima, K. Yoshihara, S. Tamura, A. Kanazawa, D. Inagaki, N. Yamamoto, T. Sato, S. Fujii, K. Numata, C. Kunisaki, M. Shiozawa, S. Morinaga, M. Akaike, Y. Rino, K. Tanaka, M. Masuda, T. Imada, *Anticancer Res.* **2010**, *30*, 2693.
[40] B. Têtu, J. Brisson, C. S. Wang, H. Lapointe, G. Beaudry, C. Blanchette, D. Trudel, *Breast Cancer Res.* **2006**, *8*, 9.
[41] S. Curran, S. R. Dundas, J. Buxton, M. F. Leeman, R. Ramsay, G. I. Murray, *Clin. Cancer Res.* **2004**, *10*, 8229.
[42] C. Gialeli, A. D. Theocharis, N. K. Karamanos, *FEBS J.* **2010**, *278*, 16.
[43] D. Grobelny, L. Poncz, R. E. Galardy, *Biochemistry* **1992**, *31*, 7152.
[44] D. E. Levy, F. Lapierre, W. Liang, W. Ye, C. W. Lange, X. Li, D. Grobelny, M. Casabonne, D. Tyrrell, K. Holme, A. Nadzan, R. E. Galardy, *J. Med. Chem.* **1998**, *41*, 199.
[45] L. Udabage, G. R. Brownlee, S. K. Nilsson, T. J. Brown, *Exp. Cell Res.* **2005**, *310*, 205.
[46] Y. Luo, M. S. Shoichet, *Nat. Mater.* **2004**, *3*, 249.
[47] F. Sabeh, R. Shimizu-Hirota, S. J. Weiss, *J. Cell Biol.* **2009**, *185*, 11.
[48] K. L. Sodek, T. J. Brown, M. J. Ringuette, *BMC Cancer* **2008**, *8*, 223.
[49] W. Guo, F. G. Giancotti, *Nat. Rev. Mol. Cell Biol.* **2004**, *5*, 816.
[50] J. A. Neff, P. A. Tresco, K. D. Caldwell, *Biomaterials* **1999**, *20*, 2377.
[51] W. A. Comisar, N. H. Kazmers, D. J. Mooney, J. J. Linderman, *Biomaterials* **2007**, *28*, 4409.